Transitions in matter triggered by intense ultrashort X-ray pulses

B. Ziaja[1,2]

in collaboration with:

Z. Jurek[1] , M.A. Malik[1], N. Medvedev[1], V. Saxena[1], S. K. Son[1], R. Thiele[1], V. Tkachenko[1], and R. Santra[1]

[1] Center for Free-Electron Laser Science, Hamburg

[2] Institute of Nuclear Physics, PAS, Kraków

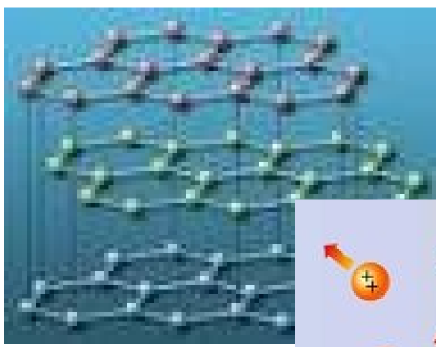

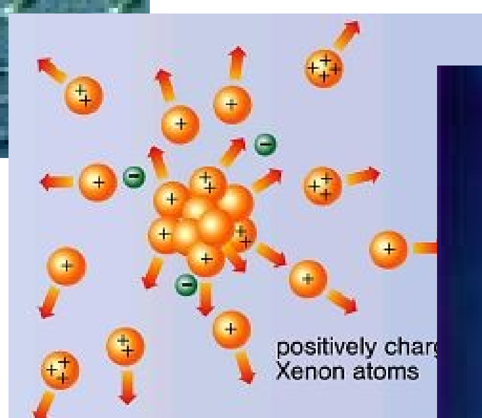

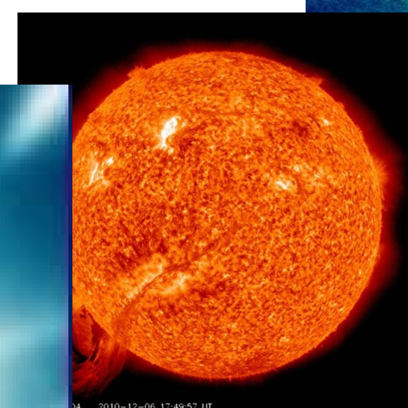

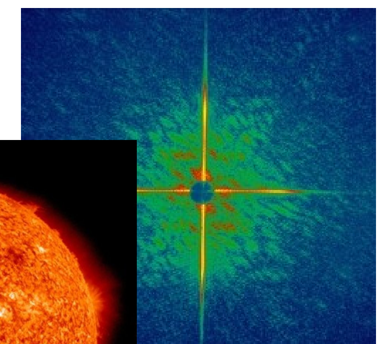

HELMHOLTZ ASSOCIATION

CFEL SCIENCE

DESY

Theory Division
at Center for Free-Electron Laser Science

The CFEL Theory Division develops theoretical and computational tools to predict the behavior of matter exposed to intense electromagnetic radiation. We employ quantum-mechanical and classical techniques to study ultrafast processes that take place on time scales ranging from 10^{-12} s to 10^{-18} s. Our research interests include the dynamics of excited many-electron systems; the motion of atoms during chemical reactions; and x-ray radiation damage in matter.

Members of the CFEL Theory Division: Y.-J. Chen, O. Geffert, Z. Jurek, Y. Hao, K. Hanasaki, A. Hanna, A. Karamatskou, Z. Li, M. A. Malik, N. Medvedev, P. K. Mishra, S. Pabst, D. Popova, R. Santra (Division Director), V. Saxena, J. M. Slowik, S.-K. Son, V. Tkachenko, O. Vendrell, B. Ziaja

3 subgroups: 'Ab-initio X-ray Physics' (R. Santra), 'Chemical Dynamics' (O. Vendrell), 'Modeling of Complex Systems' (B. Ziaja)

HELMHOLTZ
ASSOCIATION

CFEL
SCIENCE

DESY

FELs: 4th generation light sources

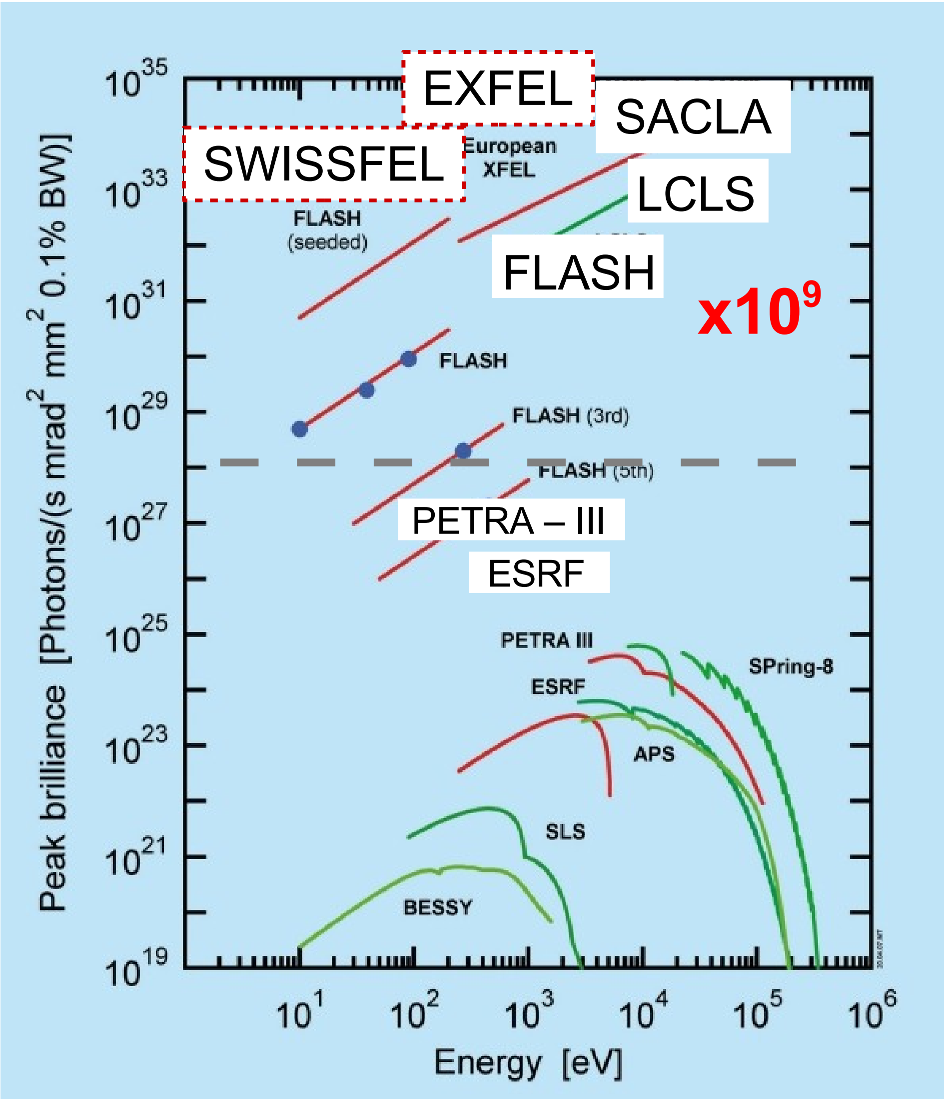

photon-science.desy.de

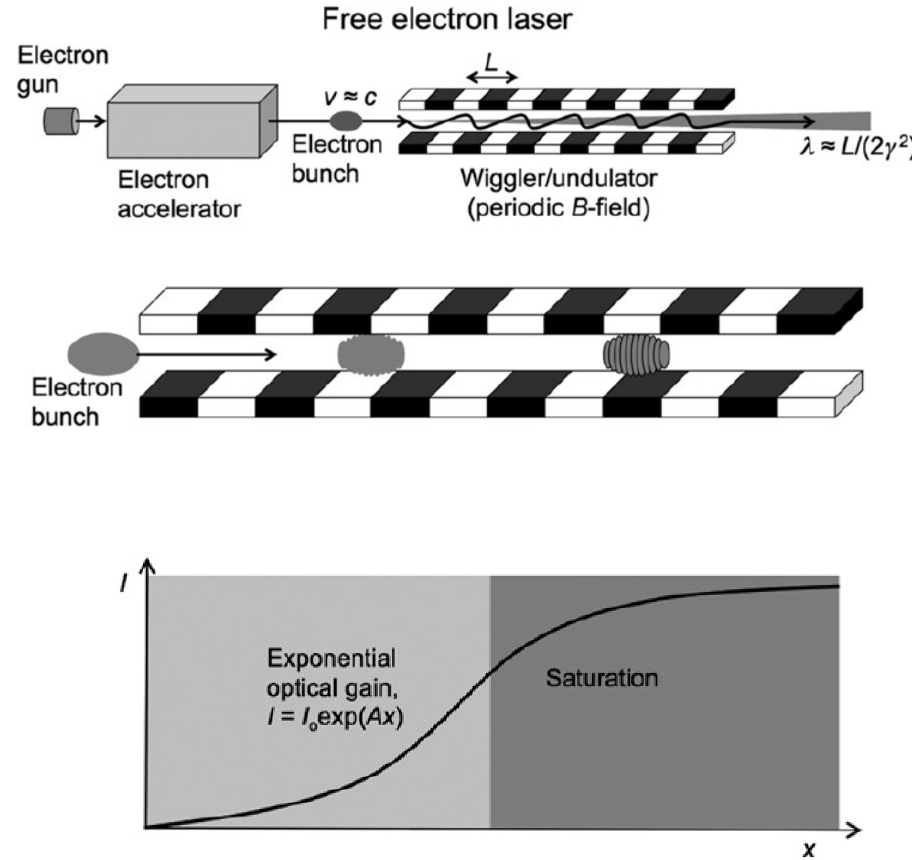

Ribic, Margaritondo, J. Phys. D **45** 213001 (2012)

Pulse duration ~ down to 10 fs
Wavelength ~ VUV- hard X-ray

[This slide courtesy of Z. Jurek]

Content

- Physical mechanisms of radiation induced dynamics within samples irradiated with soft- and hard X-rays
- Radiation-induced structural changes in irradiated solids
- Modeling of nanoplasmas created from finite systems
- Atomic processes within laser-created plasmas

HELMHOLTZ ASSOCIATION

CFEL SCIENCE

DESY

I. Physical mechanisms of radiation induced dynamics

Dynamics induced by photons of X-ray energies

Processes contributing:

- photoionizations from outer and inner shells (hard X-ray photons) with subsequent relaxation (Auger decays, fluorescence); elastic scattering of photons; Compton scattering
- collisional processes: electron impact ionization, 3-body recombination; elastic scatterings of electrons on atoms/ions
- long-range Coulomb interactions of charges with internal fields
- short-range electron-electron interaction
- modification of atomic potentials by electron screening and ion environment

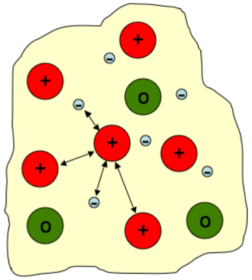

- field ionization by internal electric field
- inverse bremsstrahlung (with soft X-ray photons only)

II. Radiation-induced transitions in solids

N. Medvedev

V. Tkachenko

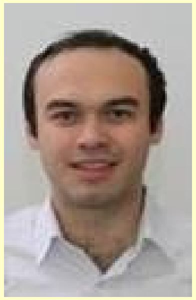

Non-equilibrium electron kinetics

Ultrafast radiation-induced electron kinetics in SiO_2

Motivated by timing tool experiments with FELs:

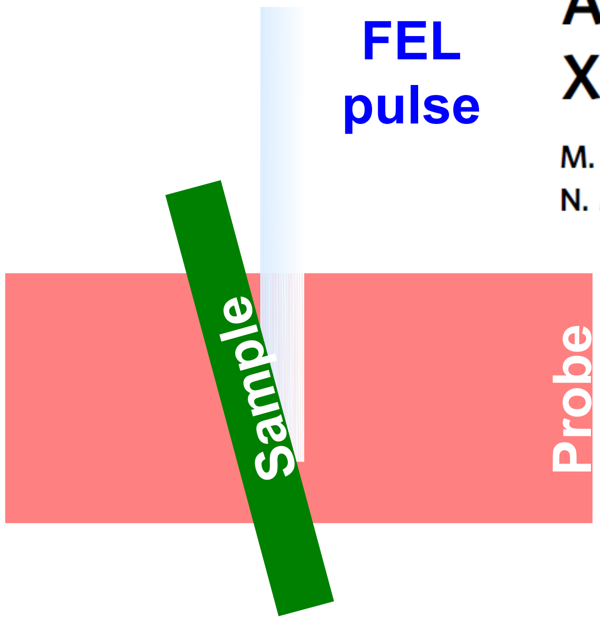

Achieving few-femtosecond time-sorting at hard X-ray free-electron lasers

M. Harmand[1†]*, R. Coffee[2], M. R. Bionta[2,3], M. Chollet[2], D. French[2], D. Zhu[2], D. M. Fritz[2], H. T. Lemke[2], N. Medvedev[4], B. Ziaja[4,5], S. Toleikis[1] and M. Cammarata[6]*

Nature Photonics 7 (2013) 215

Single-shot pulse duration monitor for EUV and X-ray pulses

R. Riedel, A. Al-Shemmary, M. Gensch, T. Golz, M. Harmand, N. Medvedev, M. J. Prandolini, K. Sokolowski-Tinten, S. Toleikis, U. Wegner, B. Ziaja, N. Stojanovic, F. Tavella

Nature Comm. 4 (2013) 1731

[This slide courtesy of N.Medvedev]

Modeling the electron kinetics

[N. Medvedev, B. Rethfeld, NJP **12** (2010) 073037]

[N. Medvedev *et al.*, PRL **107** (2011) 165003]

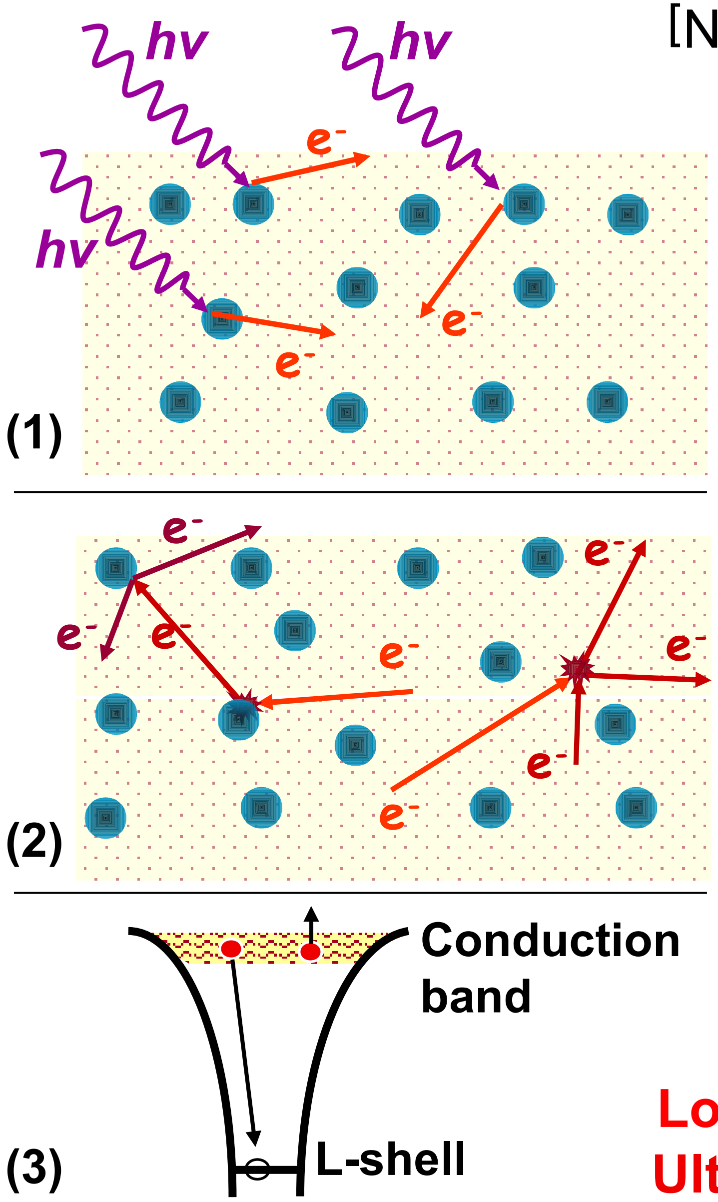

1) Photo-absorption during fs-long pulse

2) Electron redistribution:

impact ionizations, elastic scattering, electron-electron scattering

3) Auger decays of core holes (K-shell ~10 fs)

Low dose +
Ultra short timescales => electronic processes only

[This slide courtesy of N.Medvedev]

Modeling the electron kinetics

Monte Carlo approach [N. Medvedev *et al.*, Contr. Plasma Phys. 53 (2013) 347]

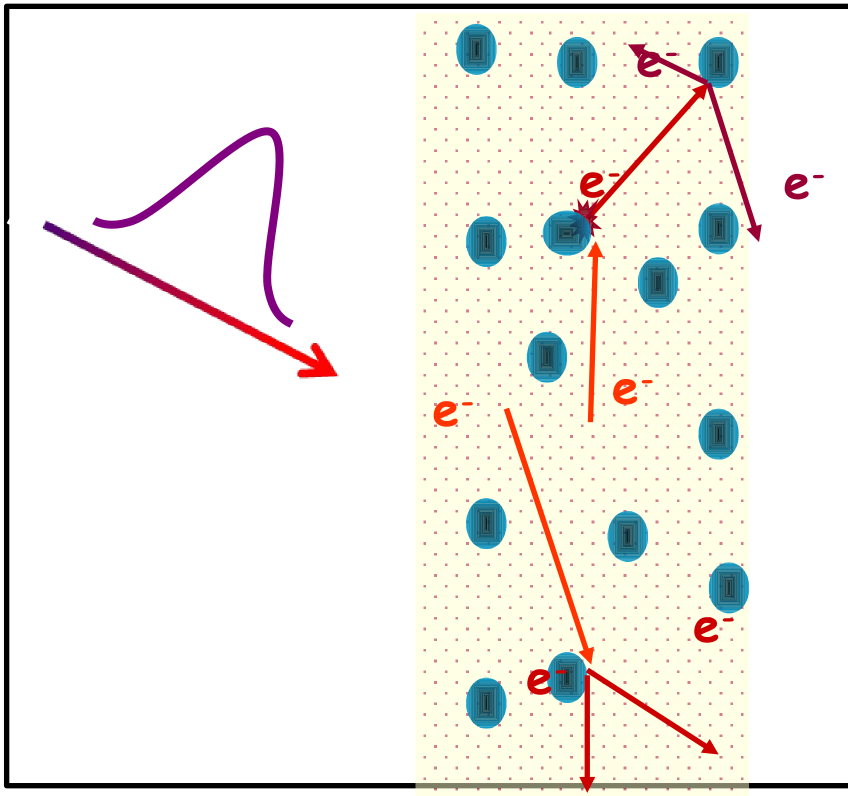

1) electron density

2) CB electron and VB holes distribution functions

Drude model:

$$n(\lambda)^2 = n_0(\lambda)^2 - \left(\frac{\omega_P}{\omega}\right)^2 \frac{1}{1 + i/(\omega\,\tau)}$$

[This slide courtesy of N.Medvedev]

Optical properties: transmission, reflection

DESY

Self-consistent semi-classical Monte-Carlo model → relaxation time τ

Results: electron density in SiO_2

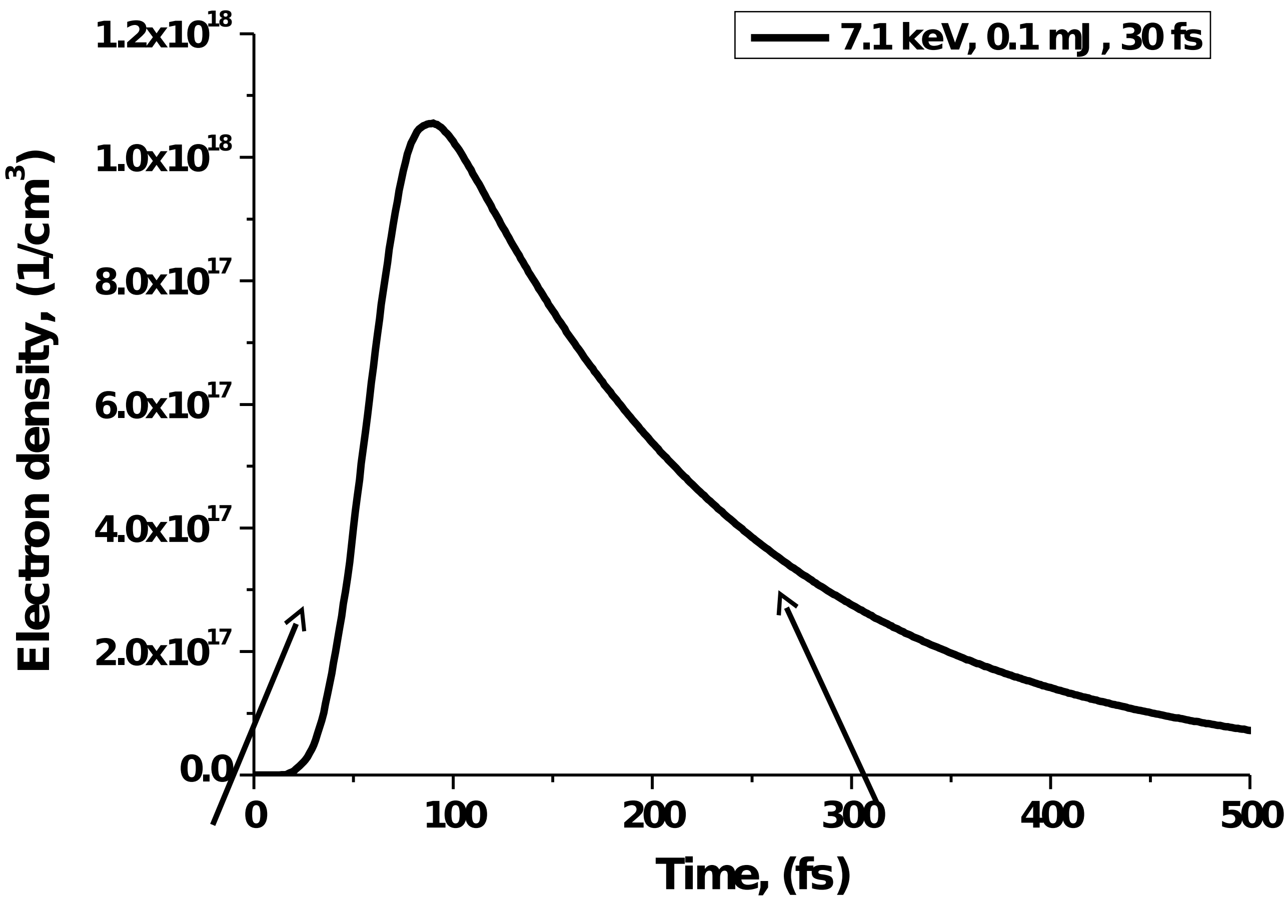

Laser pulse + secondary cascades

Electron-hole recombination via exciton mechanism

[This slide courtesy of N.Medvedev]

[N. Medvedev *et al*., Contr. Plasma Phys. 53 (2013) 347]

Results: transient transmission in SiO_2

$$n(\lambda)^2 = n_0(\lambda)^2 - \left(\frac{\omega_P}{\omega}\right)^2 \frac{1}{1 + i/(\omega\,\tau)}$$

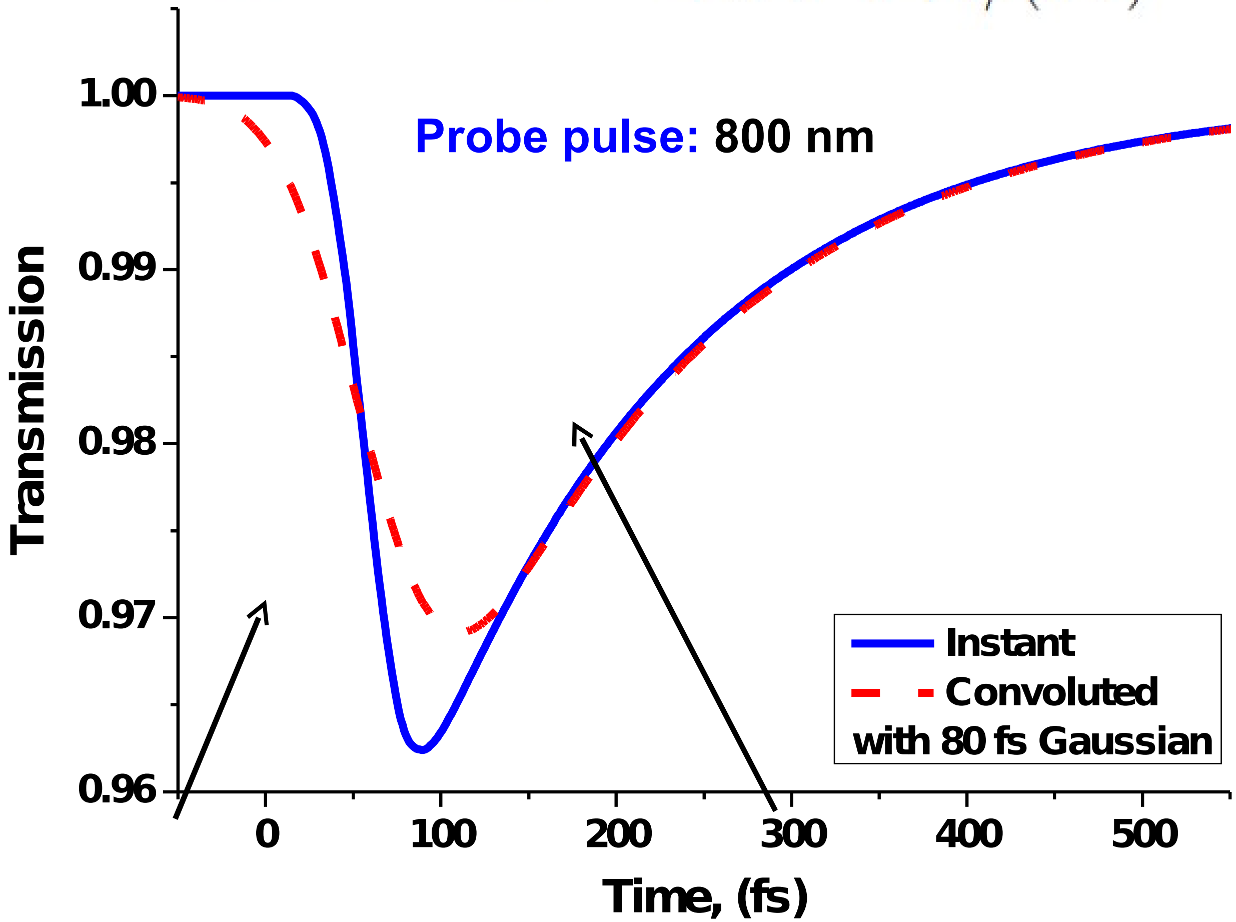

Laser pulse + secondary cascades

Electron-hole recombination via exciton mechanism

[This slide courtesy of N.Medvedev]

[N. Medvedev *et al*., Contr. Plasma Phys. 53 (2013) 347]

Results: Agreement with experimental data

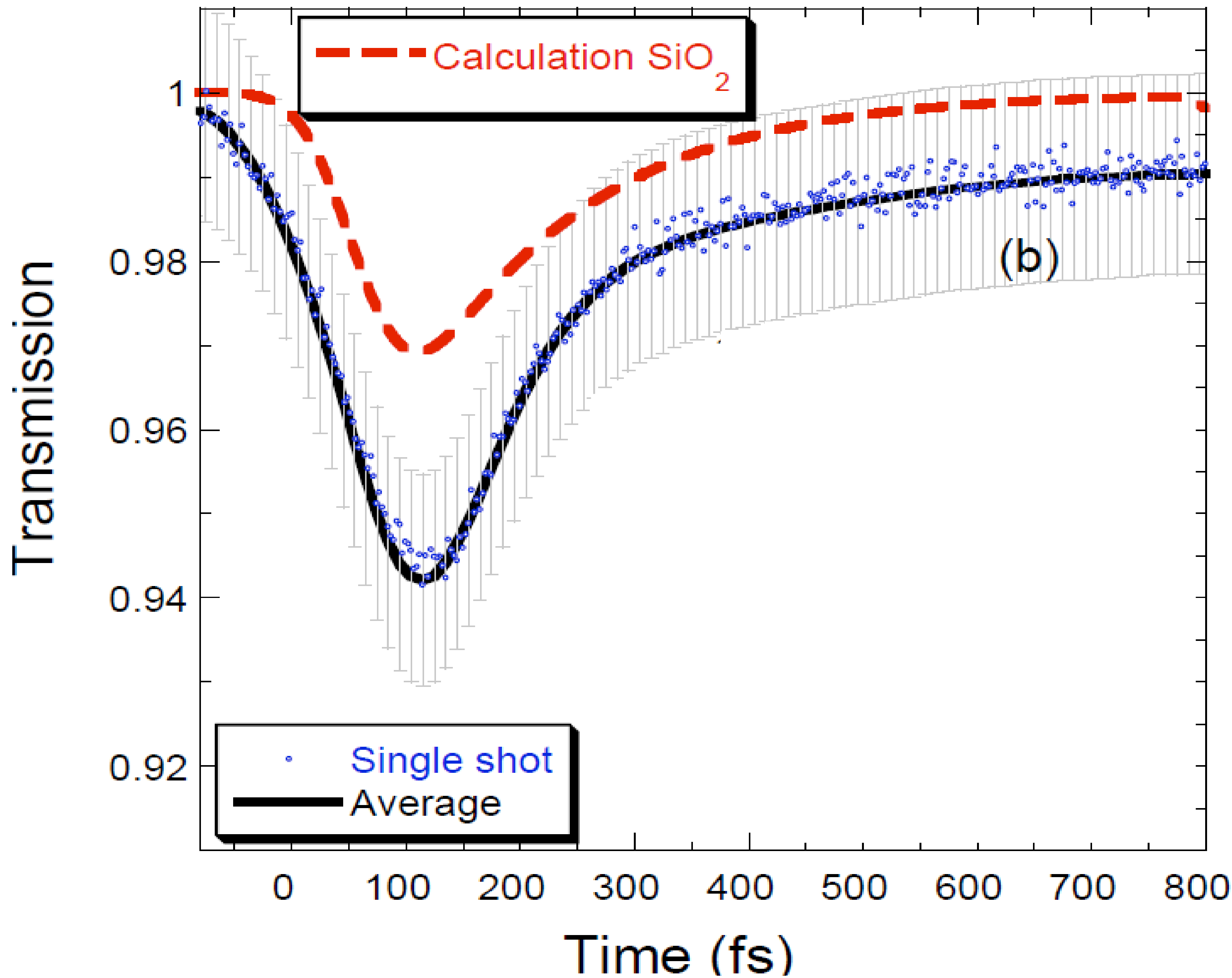

[This slide courtesy of N.Medvedev] [M. Harmand *et al.* Nature Photonics 7, 215 (2013)]

Summary for ultrafast electron kinetics in semiconductors

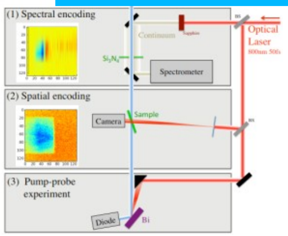

Experimental scheme allows to extract transient properties with resolution down to <10 fs

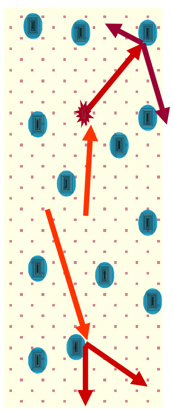

Monte Carlo code reproduces well the electron kinetics compared to experiment

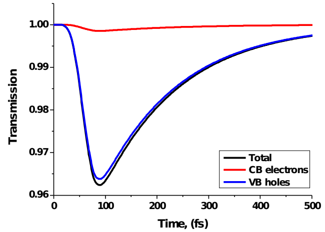

Contribution of valence holes into optical properties is dominant for X-ray irradiation

Application for other materials possible

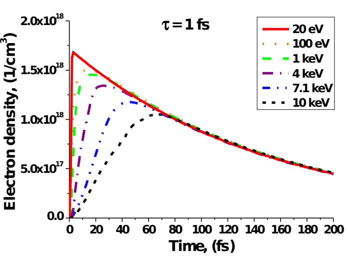

Temporal resolution limited by the formation time of secondary electron cascades

[This slide courtesy of N.Medvedev] [N. Medvedev *et al*., Contr. Plasma Phys. 53 (2013) 347]

Non-equilibrium electron kinetics
+ atomic dynamics

in Born-Oppenheimer approximation

Combined modular MC-TBMD approach to study structural changes in solids

- Molecular Dynamics (MD)
  to describe dynamics of ions and atoms
- Tight binding method / DFT
  to describe changes of band structure,
  potential energy surface
- Boltzmann approach / temperature equation
  to describe the dynamics of electrons within the valence and conduction bands
- MC approach to describe dynamics of high energy free electrons in conduction band and creation and relaxation of core holes
- Scattering / ionization rates calculated from complex dielectric function updated at each time step

[N. Medvedev, H. Jeschke, B. Ziaja; New. J. Phys. 15 (2013) 015016]

[B. Ziaja, N. Medvedev, High E. Dens. Phys. 8, (2012) 18]

TB Method and molecular dynamics (TBMD)

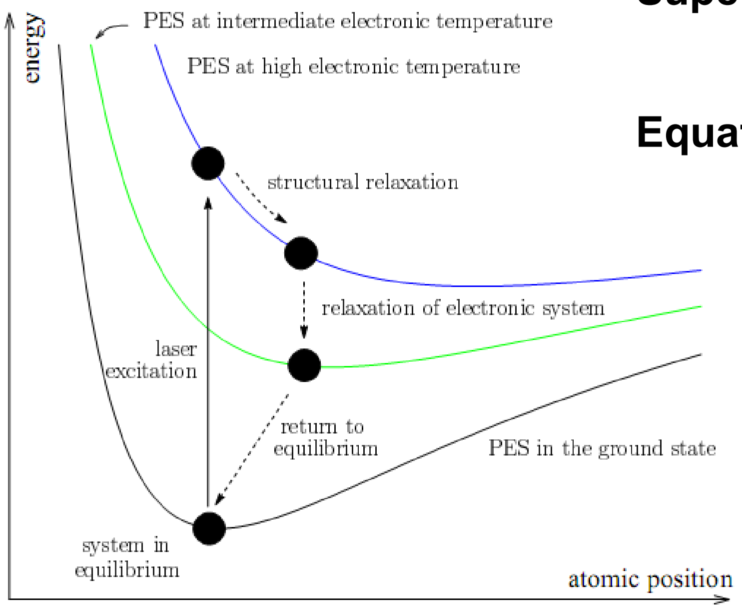

Supercell of < 1000 atoms with periodic boundary conditions

Equations of motion: $$m_k\,\ddot{\mathbf{r}}_k = -\frac{\partial\Phi(\{r_{ij}\},t)}{\partial\mathbf{r}_k}$$

Electrons **Core**

$$\Phi(\{r_{ij}(t)\},t) = \underbrace{\sum_m f(\epsilon_m,t)\epsilon_m}_{\text{Electrons}} + \underbrace{\frac{1}{2}\sum_{\substack{ij\\ j\neq i}} E_{\mathrm{rep}}(r_{ij})}_{\text{Core}}$$

$f(\epsilon_m,t)$ **- transient electron distribution function**

$\epsilon_m(\{r_{ij}(t)\}) = \langle m|H_{\mathrm{TB}}(\{r_{ij}(t)\})|m\rangle$ **- transient band structure**

[This slide courtesy of N.Medvedev]

[H. Jeschke et al. PRL 2002]

Combined MC-TBMD

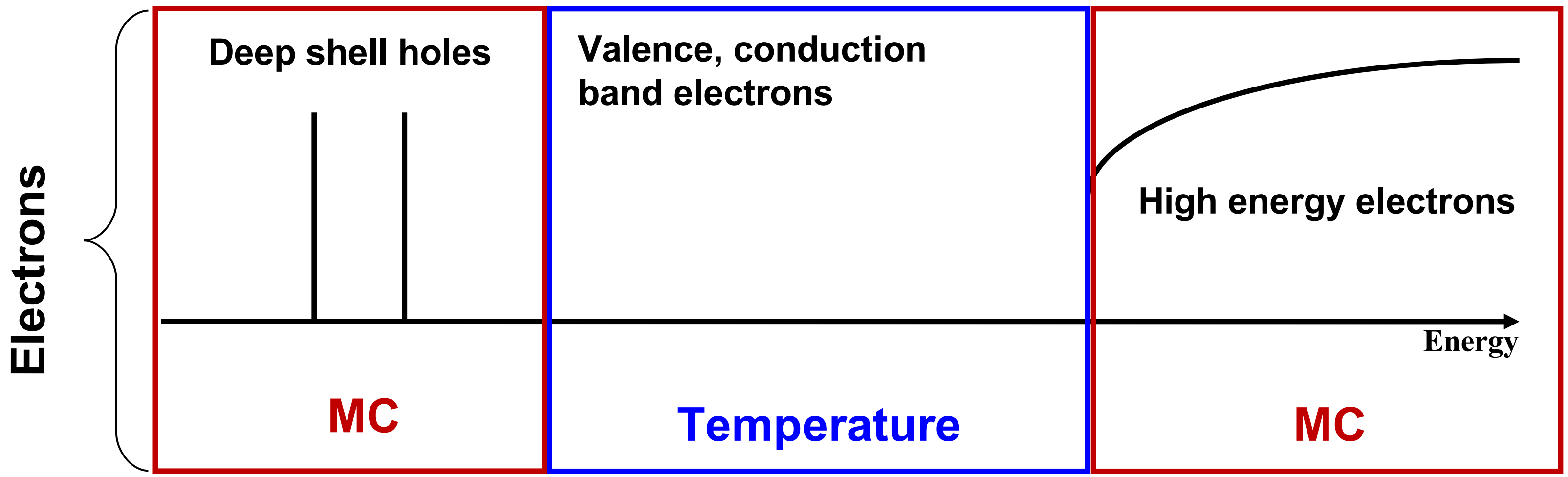

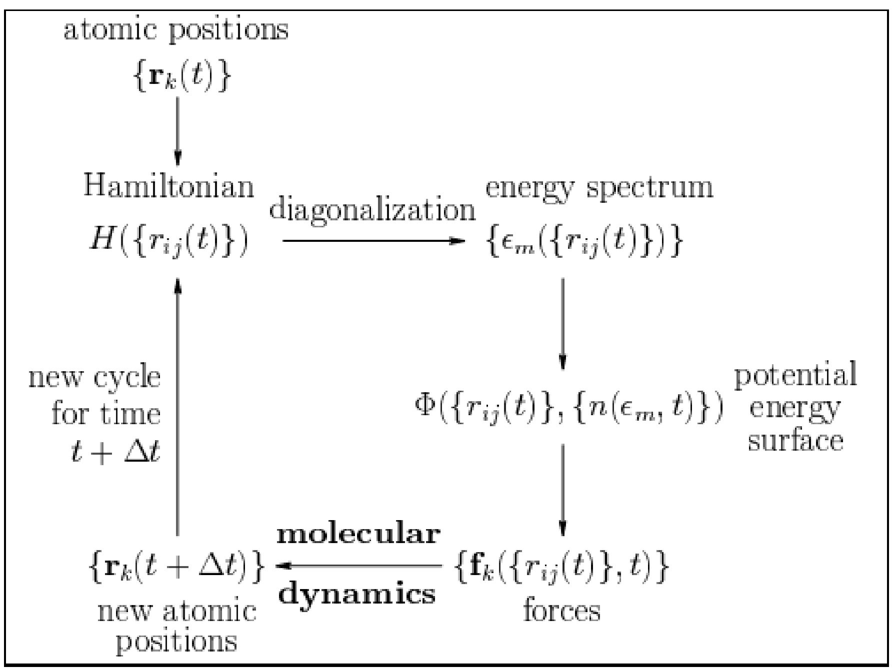

$$m_k \ddot{\mathbf{r}}_k = -\frac{\partial \Phi(\{r_{ij}\}, t)}{\partial \mathbf{r}_k}$$

Electrons — Core

$$\Phi(\{r_{ij}(t)\}, t) = \underbrace{\sum_m f(\epsilon_m, t)\epsilon_m}_{\text{Electrons}} + \underbrace{\frac{1}{2}\sum_{\substack{ij \\ j \neq i}} E_{\text{rep}}(r_{ij})}_{\text{Core}}$$

[H. Jeschke et al. PRL 2002]

[B. Ziaja, N. Medvedev, HEDP 8, 18 (2012)]

Non-adiabatic effects: [N. Medvedev, Z. Li, B. Ziaja, submitted 2014]

[This slide courtesy of N.Medvedev]

Processes considered

Photoabsorption by deep shells and VB

Scattering of fast electrons:

Deep shell-, VB and CB ionization

Auger-decays of deep-shell holes

- MC

Thermalization in VB and CB

Non-adiabatic electron-phonon coupling

- Temperature and Boltzmann Eq.

Lattice heating, atomic dynamics

Changes of band structure

Changes of scattering rates (minor effect?)

- TBMD

see [N. Medvedev et al., SPIE Proceedings 2013])

Example: Nonthermal graphitization of diamond

Photon energy 92 eV, FWHM = 10 fs

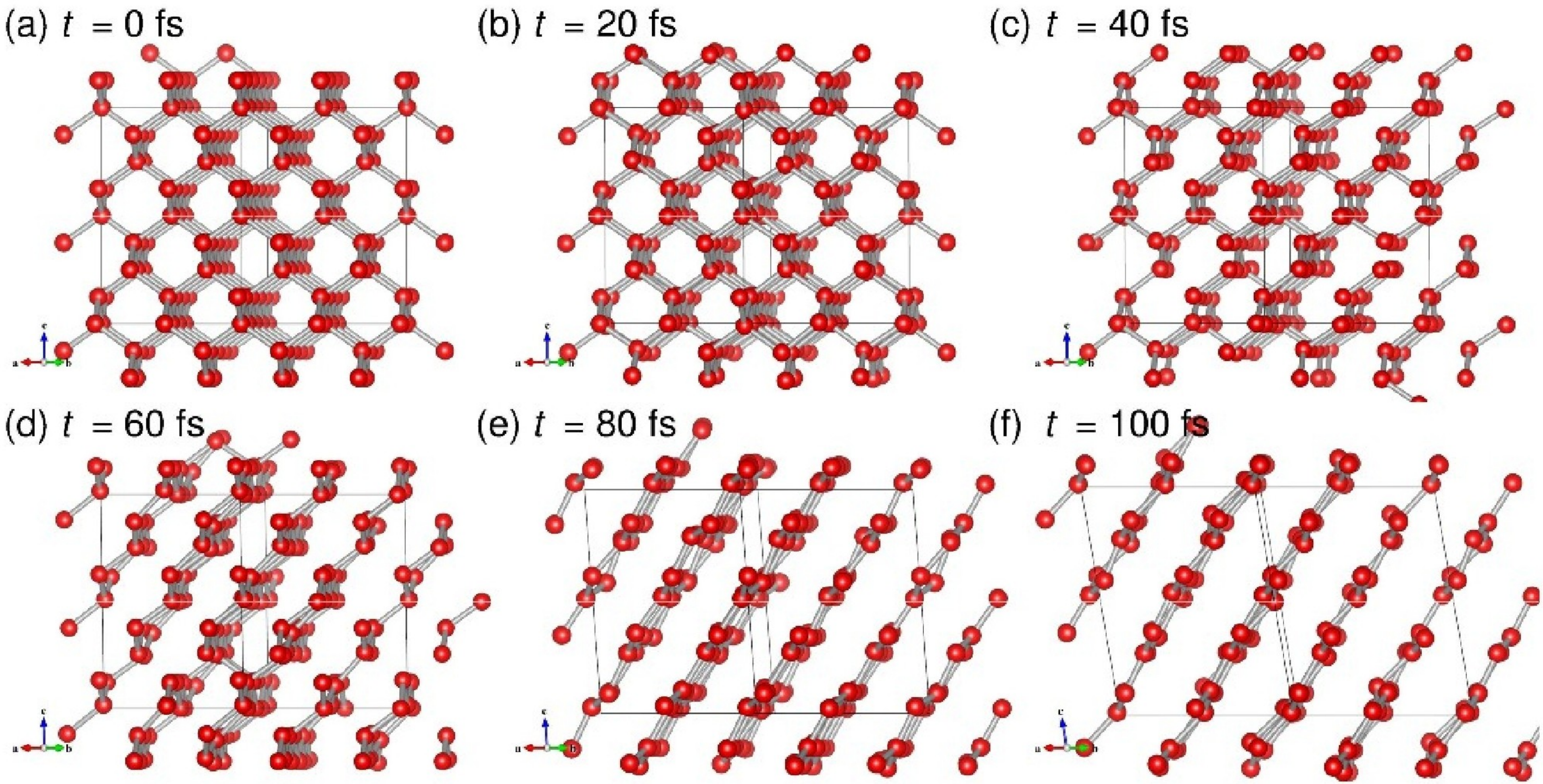

Ultrafast graphitization of diamond

[N. Medvedev, H. Jeschke, B. Ziaja, NJP 15 (2013) 015016]

[This slide courtesy of N.Medvedev]

Increase of electronic density → band gap collapse

Results: Damage threshold

Irradiated diamond turns into graphite if the fluence is high:

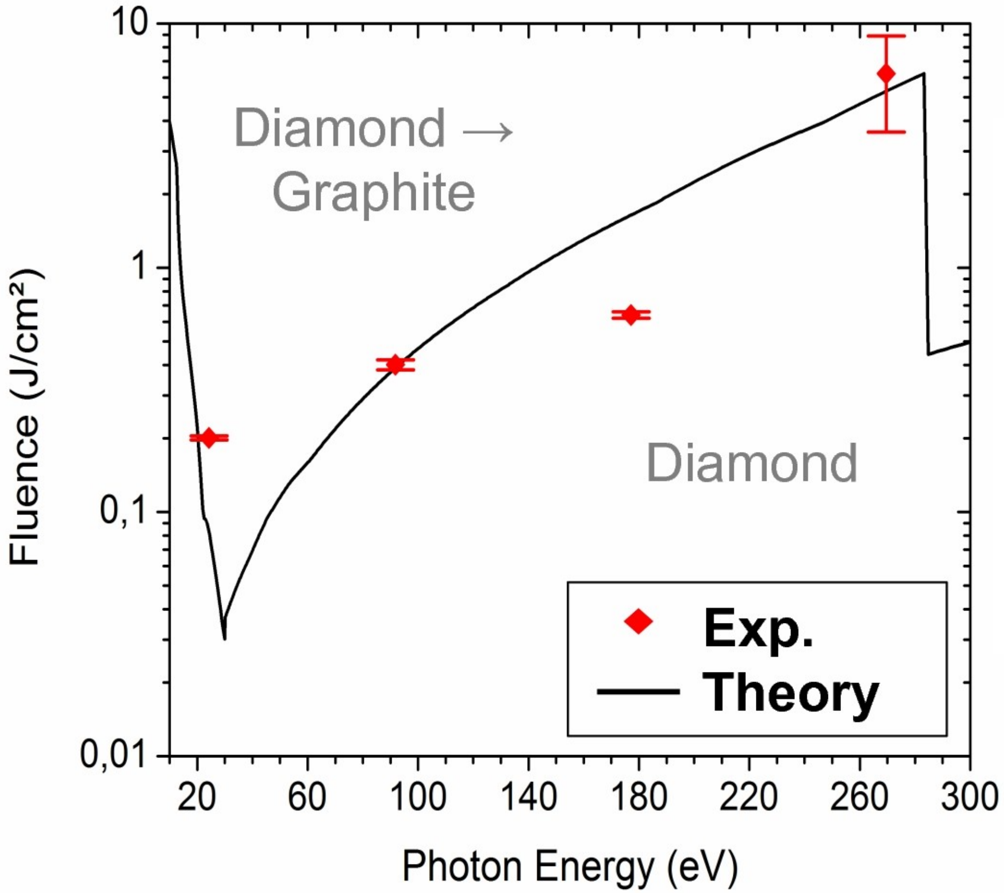

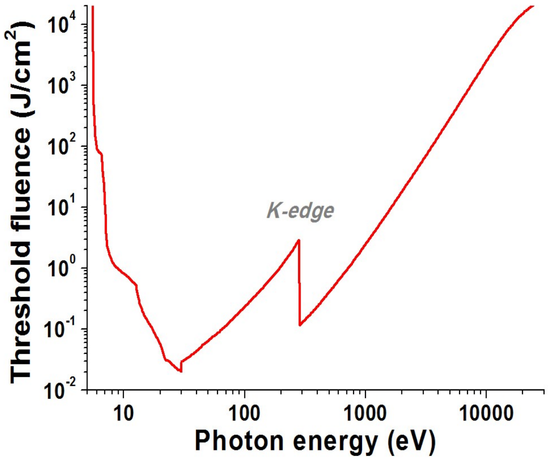

Extrapolation to hard X-rays

Damage threshold is in a good agreement with the experiments by J. Gaudin *et al.* (FLASH)

[J. Gaudin *et al.*, (2013) PRB, Rapid Comm. 88 (2013) 060101 (R)]

[N. Medvedev , H. Jeschke, BZ, PRB 88 (2013) 224304]

[This slide courtesy of N.Medvedev]

Electronic damage induced by a covering high-Z material

Damage due to the presence of another material:

e.g., 200 nm thick layer of tungsten [F. Uhlen et al. Opt. Exp.21 (2013) 8051]

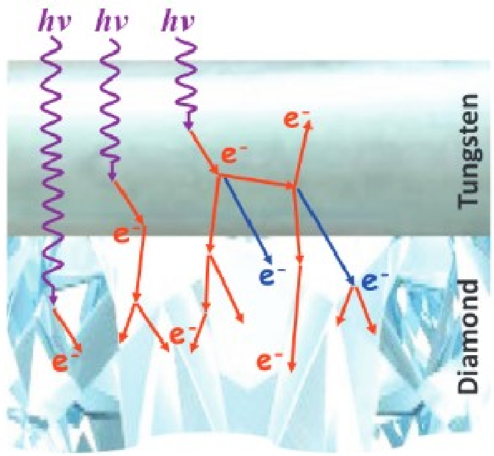

FIG. 7. (Color online) Schematic picture of the multilayer tungsten-diamond structure, irradiated with a laser pulse. The violet lines represent photons ($h\nu$), the red arrows stand for photoelectrons and secondary electrons (marked with e^-), and the blue arrows represent Auger electrons.

TABLE I. Comparison of photoabsorption in diamond with the energy deposition made by electrons from the 200-nm tungsten layer put on top of diamond. F denotes the fluence of the incoming laser pulse, $D_{ph}(C)$ is the photoabsorbed dose in diamond, and $D_e(C)$ is the dose deposited in diamond by the electrons from tungsten. For comparison, the last column shows the calculated damage threshold in diamond.

F (J/cm^2)	$D_{ph}(C)$ (eV/atom)	$D_e(C)$ (eV/atom)	Damage threshold (eV/atom)
59	0.027	0.66	
99	0.046	1.19	0.7
220	0.10	2.65	

Electrons produced in tungsten travel into diamond, increasing damage within diamond

↓

Lower damage threshold for diamond

↓

Radiation dose remaining in tungsten still sufficient to evaporate tungsten layer

[N. Medvedev , H. Jeschke, BZ, PRB 88 (2013) 224304]

Non-equilibrium electron kinetics
+ atomic dynamics

beyond Born-Oppenheimer approximation

↓

electron-phonon coupling included

Preliminary: Silicon amorphises

$\hbar\omega$ = 92 eV, FWHM = 10 fs, 2.5 eV/atom

Z. Li

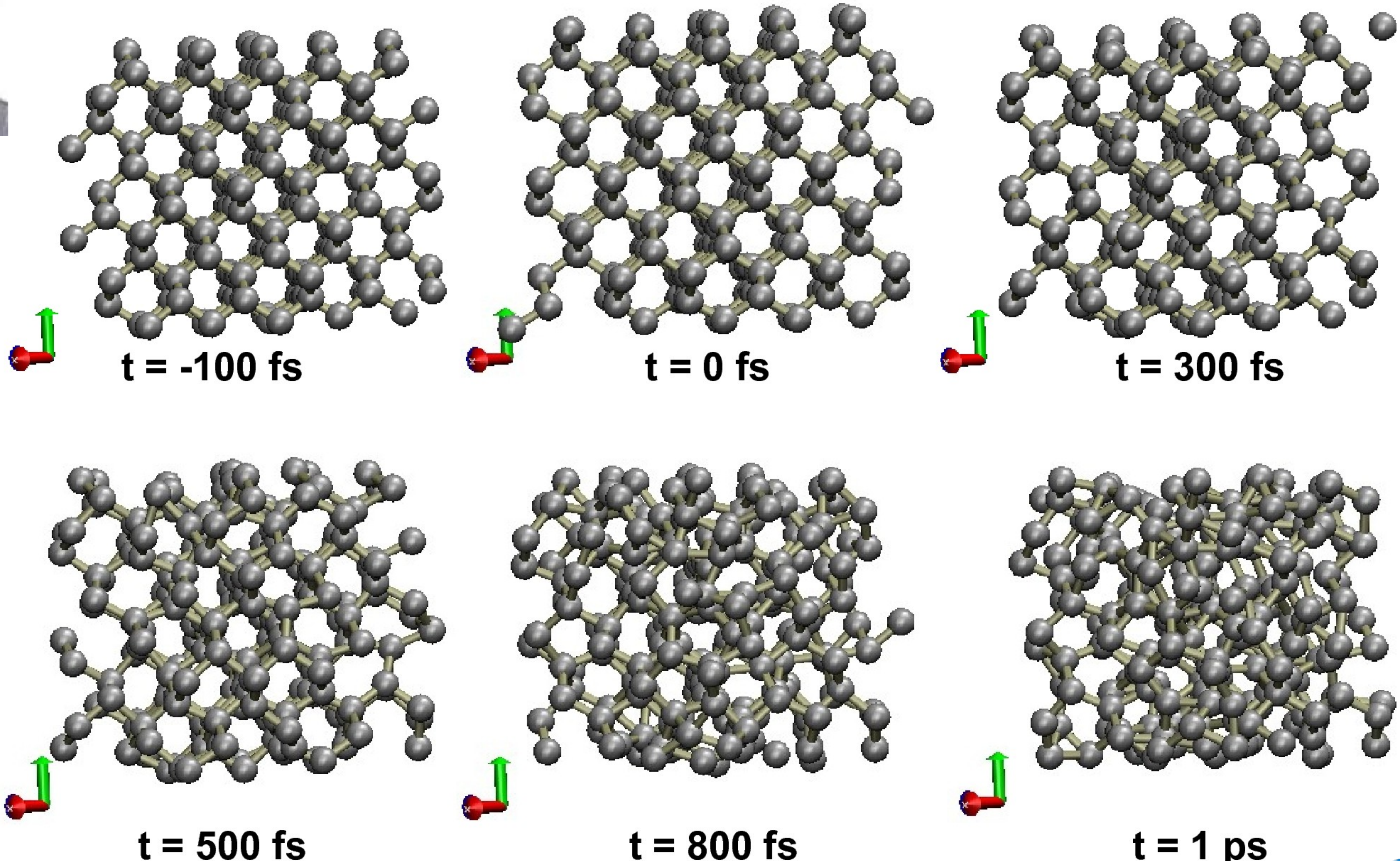

Description of ps-long transitions in irradiated silicon requires going beyond the Born-Oppenheimer approximation. The transitions are an interplay of nonthermal and thermal effects → [N. Medvedev, Z. Li, B. Ziaja, submitted]

[This slide courtesy of N.Medvedev]

Summary for MC-TBMD model

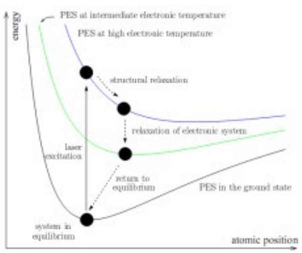

- New **hybrid MC-TBMD** model was developed to follow structural transitions within irradiated solids at low pulse fluence

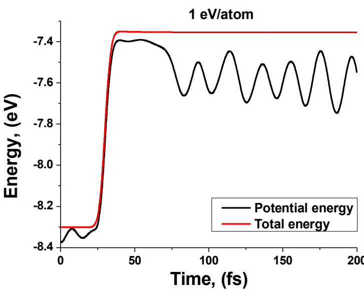

- Transition from **diamond to graphite** after FLASH irradiation within ~100 fs. In **silicon** within ~1 ps.

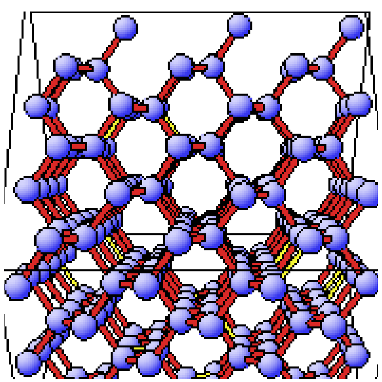

- **Nonthermal (C,Si) and thermal (Si)** melting of solids after VUV-XUV irradiation observed in simulations.

- **Experimental verification** for diamond damage thresholds positive. Time-resolved experiment under consideration.

[This slide courtesy of N.Medvedev]

III. Modeling of nanoplasmas created from finite systems

Zoltan Jurek

Muhammad Malik

Robin Santra

Particle approach

Modeling with molecular dynamics method

In-house Molecular Dynamics code XMDYN → see talk by Zoltan Jurek ...

Successfully applied to strongly bound molecular system, C_{60} in the limit of single photoionization (synchrotron) ...

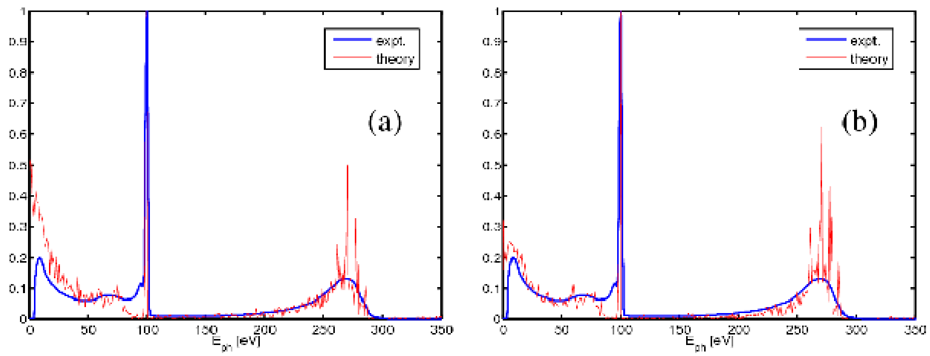

Electron kinetic energy spectrum

... and multiple ionization (LCLS)
→ Coulomb explosion

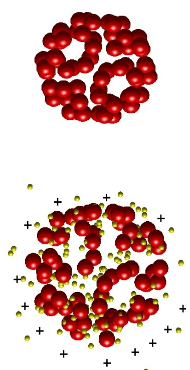

... for noble gas clusters (SACLA)

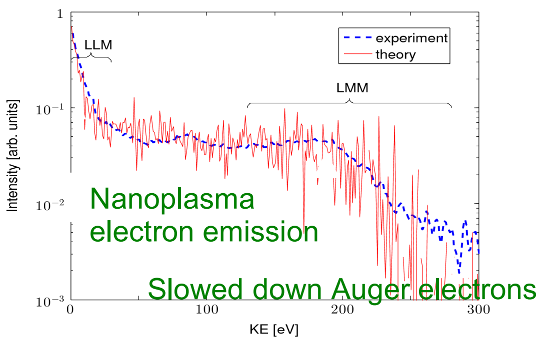

Transport approach

Transport approach

Statistical description of a classical system in terms of density functions $\rho(\mathbf{r}, \mathbf{v}, t)$ in phase space

$\rho(\mathbf{r}, \mathbf{v}, t) d^3r\, d^3v$ is a number of particles located at $\mathbf{r}$ of velocity $\mathbf{v}$ in the phase space element $d^3r\, d^3v$

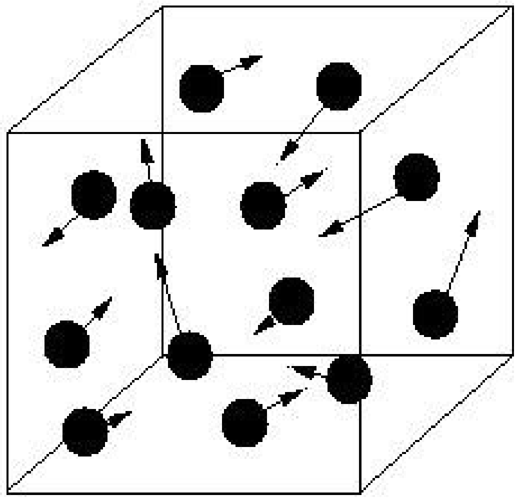

$$\int \rho(\mathbf{r}, \mathbf{v}, t) d^3r\, d^3v = N(t)$$

$$\int \rho(\mathbf{r}, \mathbf{v}, t)\, d^3r = n(\mathbf{v}, t)$$

$$\int \rho(\mathbf{r}, \mathbf{v}, t)\, d^3v = n(\mathbf{r}, t)$$

Solving Boltzmann equations

The general coupled Boltzmann equations for electron, $\rho^{(e)}(\mathbf{r},\mathbf{v},t)$, and ion densities, $\rho^{(i)}(\mathbf{r},\mathbf{v},t)$, where $i = 0, 1, \ldots, N_J$ denotes the ion charge, and N_J is the maximal ion charge in the system are:

$$\partial_t \rho^{(e)}(\mathbf{r},\mathbf{v},t) + \mathbf{v}\cdot\partial_{\mathbf{r}}\rho^{(e)}(\mathbf{r},\mathbf{v},t) + \frac{e}{m}\left(\mathbf{E}(\mathbf{r},t) + \mathbf{v}\times\mathbf{B}(\mathbf{r},t)\right)\cdot\partial_{\mathbf{v}}\rho^{(e)}(\mathbf{r},\mathbf{v},t) = \Omega^{(e)}(\rho^{(e)},\rho^{(i)},\mathbf{r},\mathbf{v},t),$$

$$\partial_t \rho^{(i)}(\mathbf{r},\mathbf{v},t) + \mathbf{v}\cdot\partial_{\mathbf{r}}\rho^{(i)}(\mathbf{r},\mathbf{v},t) - \frac{ie}{M}\left(\mathbf{E}(\mathbf{r},t) + \mathbf{v}\times\mathbf{B}(\mathbf{r},t)\right)\cdot\partial_{\mathbf{v}}\rho^{(i)}(\mathbf{r},\mathbf{v},t) = \Omega^{(i)}(\rho^{(e)},\rho^{(i)},\mathbf{r},\mathbf{v},t).$$

These equations include the total electromagnetic force acting on ions and electrons. Collision terms, $\Omega^{(e,i)}$, describe the changes of the electron/ion densities of velocities $(\mathbf{v}, \mathbf{v}+\mathbf{dv})$ measured at the positions $(\mathbf{r}, \mathbf{r}+\mathbf{dr})$ with time. These changes are due to short-range processes, e. g. collisions, photoabsorptions. The number of processes involved in the sample dynamics depends on the radiation wavelength.

Application of Boltzmann code for X-ray resonant magnetic scattering

- **Described breakdown of the X-ray resonant magnetic signal during intense pulses of XUV radiation**

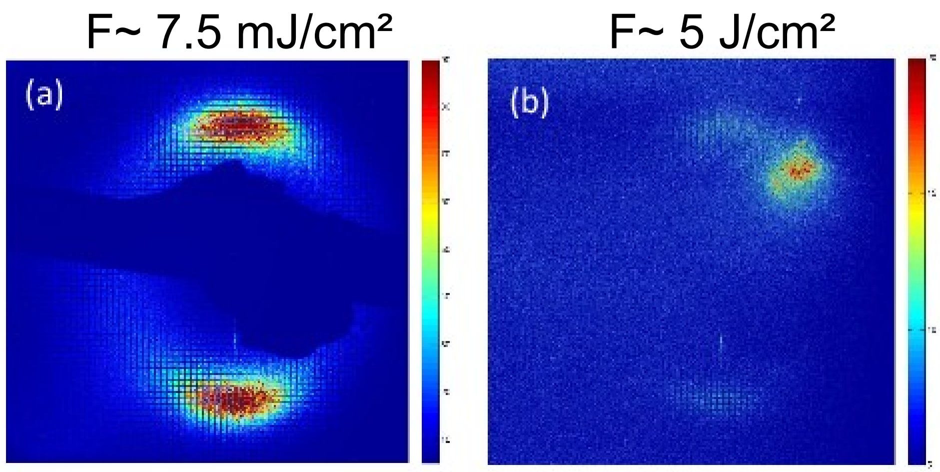

An X-ray induced breakdown of the resonant magnetic scattering channel during the pulse duration was observed at fluences of 5 J/cm2 in single shot resonant magnetic scattering experiments of Co/Pt multilayer systems using 100 fs long ultra-intense pulses from a XUV free-electron laser. Simultaneously, the speckle contrast of the high fluence scattering pattern was significantly reduced. We performed simulations of the non-equilibrium evolution of the Co/Pt multilayer system during the XUV pulse duration. We found that the electronic state of the sample was strongly perturbed during the first few femtoseconds of exposure leading to an ultrafast quenching of the resonant magnetic scattering mechanism.

[L. Mueller et al., PRL 110 (2013) 234801]

IV. Atomic processes within laser-created plasmas and warm-dense matter

R. Santra

S. K. Son

R. Thiele

In collaboration with 'Ab-Initio X-ray Physics' group within CFEL Theory Division: R. Santra and S. K. Son.

Effect of screening by charges within plasma on atomic potential

Physical picture:

atom or ion confined within a charged environment sees the fields of external charges. This modifies its atomic energy levels and interaction rates

↓

HFS approach:
central atom/ion with a screening-modified atomic potential

[R. Thiele, S. K. Son, B. Ziaja, R. Santra, PRA 86 (2012) 033411]

Effect of screening by charges within plasma on atomic potential

1. Standard Hartree-Fock Slater (HFS) approach [redacted]

Effective single-electron Schrödinger equation

$$\left[-\frac{1}{2}\nabla^2 + V_{\text{eff}}(\mathbf{r})\right]\psi(\mathbf{r}) = \varepsilon\psi(\mathbf{r})$$

Effective potential in unscreened HFS approach

$$V_{\text{eff}}^{HFS}(\mathbf{r}) = -\frac{Z}{r} + \int \frac{\rho(\mathbf{r}')}{|\mathbf{r}-\mathbf{r}'|}\,\mathrm{d}^3r' + V_x(\mathbf{r})$$

Electron density

$$\rho(\mathbf{r}) = \sum_i^{N_{elec}} \psi_i^\dagger(\mathbf{r})\psi_i(\mathbf{r})$$

Slater exchange potential

$$V_x(\mathbf{r}) = -\frac{3}{2}\left[\frac{3}{\pi}\rho(\mathbf{r})\right]^{1/3}$$

[1] J. C. Slater, Phys. Rev. **81**, 385 (1951)

[2] S.-K. Son, L. Young, and R. Santra, Phys. Rev. A **83**, 033402 (2011)

[This slide courtesy of R. Thiele]

Effect of screening by charges within plasma on atomic potential

2. HFS model at finite temperature ('Average-atom model')

HFS potential inside the Wigner-Seitz sphere with r_s

$$V(\mathbf{r}) = \begin{cases} -\dfrac{Z}{r} + \displaystyle\int_{r' \leq r_s} d^3 r' \, \frac{\rho(\mathbf{r}')}{|\mathbf{r} - \mathbf{r}'|} + V_{\mathrm{HFS}}[\rho(\mathbf{r})] & \text{for } r \leq r_s, \\ V(r_s) & \text{for } r > r_s, \end{cases}$$

with the Wigner-Seitz radius $r_s = (3/4\pi n)^{1/3}$

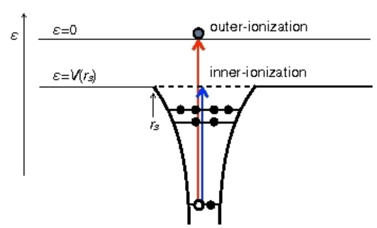

Electronic density $\rho(\mathbf{r}, T)$

$$\rho(\mathbf{r}, T) = \sum_p |\psi_p(\mathbf{r})|^2 \, n_p(\mu, T) = \sum_p |\psi_p(\mathbf{r})|^2 \, \frac{1}{1 + e^{(\varepsilon_p - \mu)/T}}$$

However, with the average-atom model we cannot obtain individual electronic configurations!

[1] N. Mermin, Annals of Physics **21**, 99 (1963)
[2] B. F. Rozsnyai, Phys. Rev. A **5**, 1137 (1972)
[3] W. R. Johnson, J. Nilsen, and K. T. Cheng, Phys. Rev. E **86**, 036410 (2012)
[4] S.-K. Son, R. Thiele, B. Ziaja, and R. Santra, in preparation (2013)

DESY

[This slide courtesy of R. Thiele]

Effect of screening by charges within plasma on atomic potential

The partition function of the grand-canonical ensemble is given by

$$Y = \mathrm{Tr}\{e^{-\beta(\hat{H}-\mu\hat{N})}\}, \qquad \text{(A1)}$$

Then, the probability of finding one specific configuration of $\{n_p\}$ is →

$$P_{\{n_p\}} = \frac{1}{Y} e^{-\beta\sum_p(\varepsilon_p-\mu)n_p} = \prod_{p=1}^{\infty} \frac{e^{-\beta(\varepsilon_p-\mu)n_p}}{1+e^{-\beta(\varepsilon_p-\mu)}}. \qquad \text{(A4)}$$

Probability of a fixed configuration n_b

$$P_{[n_b]} = \sum_{\{n_p\}=\{n_b;n_{p'}\}} P_{\{n_p\}}.$$

↓

Probability of a charge state Q

$$P_Q = \sum_{\substack{(n_1,\cdots,n_{N_b}) \\ n_1+\cdots+n_{N_b}=Z-Q}} P_{(n_1,\cdots,n_{N_b})}.$$

↓

Average charge state at temperature T

$$\bar{Q} = Z - \sum_{p=1}^{B} \frac{1}{e^{\beta(\varepsilon_p-\mu)}+1},$$

TWO-STEP HFS MODEL:
FORMAL FOUNDATIONS

[S.K. Son et al., PRX 4, 031004 (2014)]

Effect of screening by charges within plasma on atomic potential

It results in a fixed-configuration calculation:

Average-atom HFS calculation → free-electron density, ρ_f , at temperature T (including only continuum orbitals)

Bound electron density ρ_b ← constructed with fixed electronic configurations from bound orbitals

Total electron density, $\rho_t = \rho_b + \rho_f$ is then used for self-consistent HFS calculations, with ρ_f fixed.

[S.K. Son et al., PRX 4, 031004 (2014)]

Effect of screening by charges within plasma on atomic potential

Kα emission: S.M. Vinko *et al.*, Nature 482, 59 (2012)

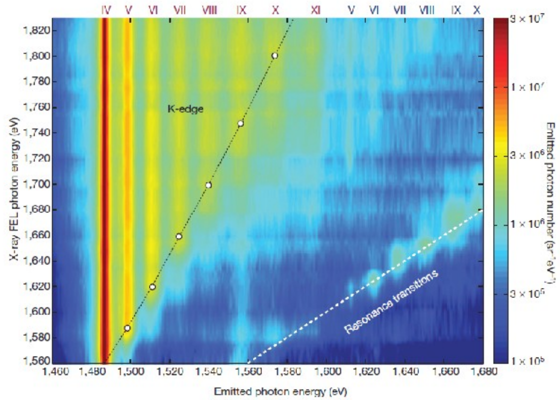

Figure 1 | Spectrally resolved Kα emission as a function of the X-ray FEL excitation photon energy. The colour coding (bar on right) refers to the emission intensity on a logarithmic scale. Roman numerals (top) indicate the charge state of the emission peak: red, for states with a single K-shell hole; blue, for states with a double K-shell hole. Peaks around the resonance line (dashed white line, indicating where the FEL photon energy equals the emitted photon energy) correspond to emission from resonantly pumped K–L transitions. Open circles, K edges for the various charge states calculated in the SCFLY code, which includes the ionization potential depression in the dense plasma according to a modified version of the Stewart-Pyatt model[21,22].

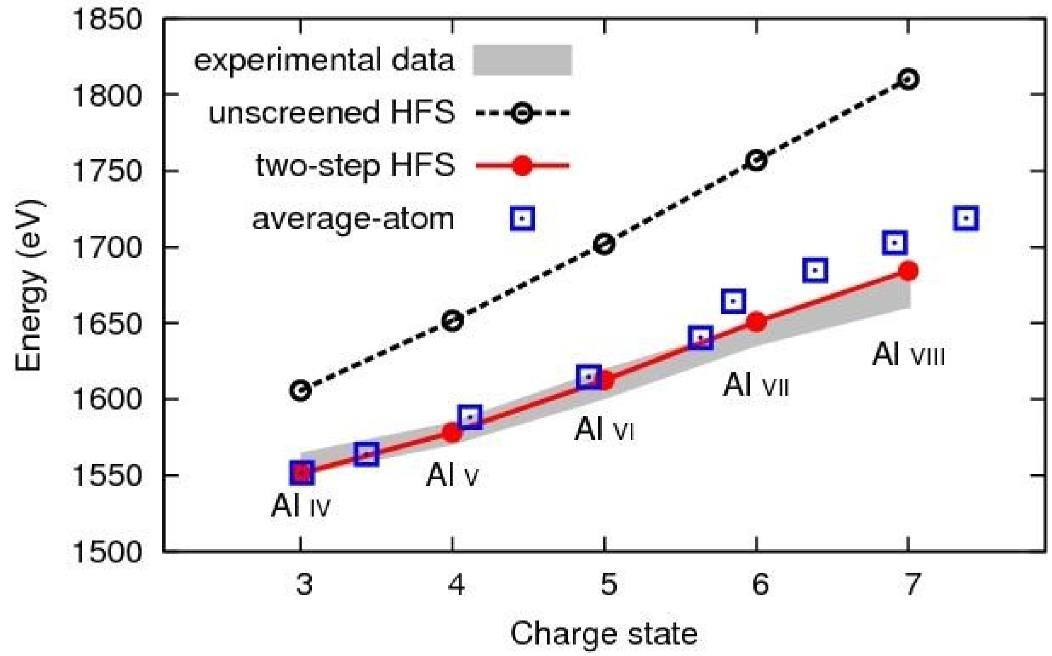

FIG. 2. (color online) K-shell thresholds for aluminum as a function of the charge state calculated with the two-step HFS model. The average-atom results from the first step only are plotted as a function of the average charge state. The Vinko et al. data are taken from Ref. [22]. The unscreened HFS results correspond to the calculations for isolated ions.

Strongly to weakly coupled plasma:

Good agreement of the two-step model with the solid-density Al plasma data!

[Vinko et al., Nature 482 (2012) 59]

Effect of screening by charges within plasma on atomic potential

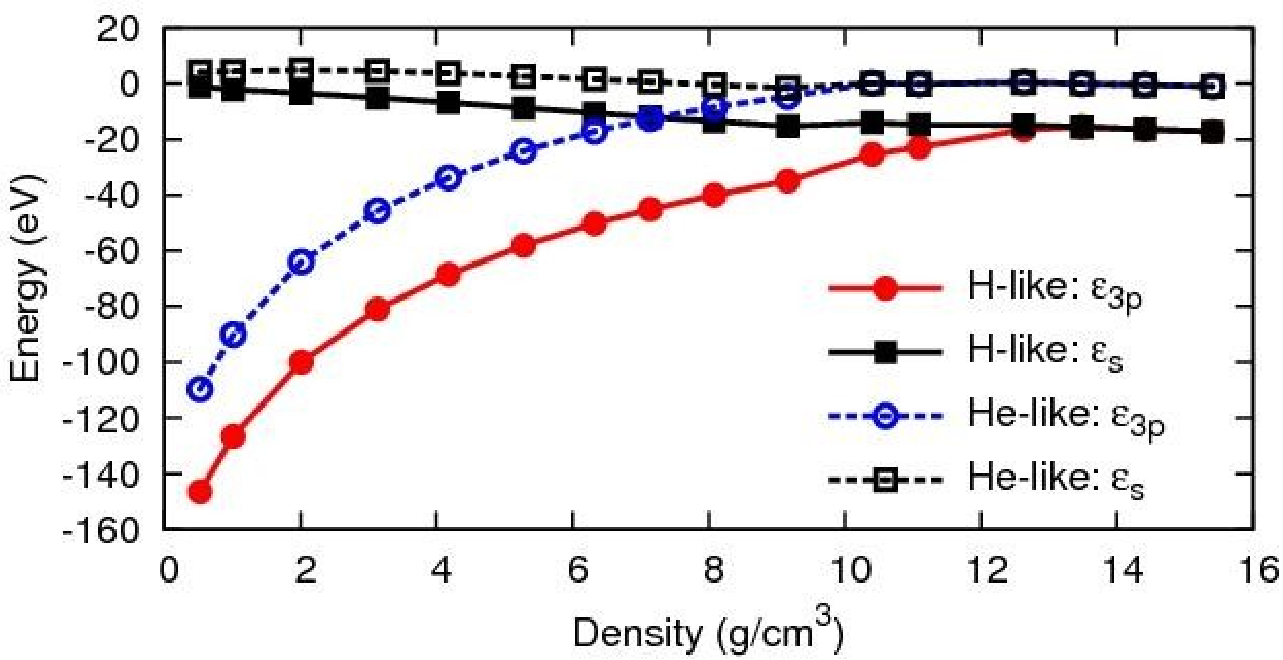

FIG. 4. (color online) The potential tail (ε_s) and 3p orbital energy (ε_{3p}) of H-like and He-like Al as a function of the solid density at $T = 700$ eV.

Very weakly coupled plasma: predicted merging of 3p state with continuum is in good agreement with the experimental results on compressed Al

[Hoarty et al., PRL 110 (2013) 265003]

Summary on investigation of screening by charges within plasma

- 'Standard' plasma models: Stewart-Pyatt and Ecker-Kroell models fail to describe all recently available experimental data on atomic level shifts

- First principle two-step finite-temperature HFS model is able to describe these level shifts with a good acccuracy both within strongly and weakly coupled plasma

[Hoarty et al., PRL 110 (2013) 265003] [Vinko et al., Nature 482 (2012) 59]

↓ ↓ ↓

IPD estimates from the two-step HFS model included into FLYCHK code (H.K. Chung) ...

[S.K. Son et al., PRX 4, 031004 (2014)]

DESY

Alternative way to measure effect of screening by charges within plasma

The above hard-X-ray based method uses the information encoded in fluorescence spectra and is restricted to the inner shell atomic levels.

We proposed a complementary way of probing the plasma screening effect. The proposed photoelectron spectroscopy method can probe the outer-shell atomic levels in nanoplasmas.

Pump pulse creates a nanoplasma ... Destructive probe pulse probes nanoplasma in the regime of massively parallel ionization

[B. Ziaja et al., J. Phys. B 46 (2013) 164009] → experiment at FLASH under discussion

Summary

- **Radiation-induced transitions in solids, modeling of nanoplasmas created from finite systems, and atomic processes within laser-created plasmas were discussed**
- **Various processes are contributing to radiation induced dynamics, depending on the FEL pulse fluence and its wavelength. They may result in: structural changes → sample 'destruction'**
- **Various theoretical approaches → various codes applied ...**

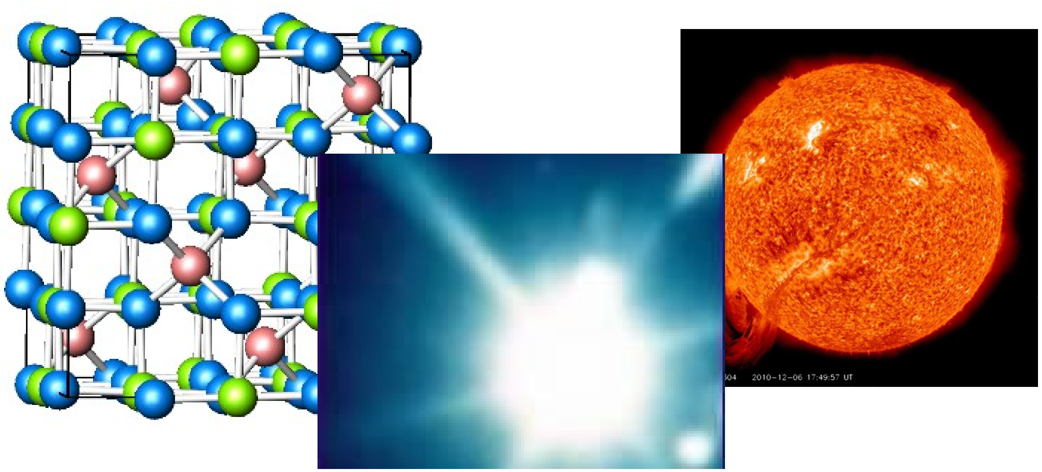

Summary of codes

- Atomic data and transitions rates from XATOM package (R. Santra & S. K. Son)
- Transport approach → Boltzmann code: irradiation of atomic clusters with VUV and soft X-ray photons (B. Ziaja) → extension to hard X-ray regime underway
- Hybrid MC- TBMD approach → modeling of structural changes in irradiated solids → applied to describe nonthermal melting and recently thermal melting in semiconductors (N. Medvedev)
- Monte Carlo model to follow ultrafast electron kinetics in X-rays irradiated solids (N. Medvedev); an element-flexible fast version available lately → transient optical properties, also beyond Drude model
- Molecular Dynamics code to follow classical ion and electron dynamics in X-ray irradiated clusters and macromolecules (Z. Jurek)→ long-timescale hydrodynamic extension, XHYDRO (V. Saxena) and on-the-fly coupling to XATOM (S. K. Son)

Thanking our external collaborators...

Ch. Bostedt (LCLS), T. Moeller (TU Berlin)

H. Chapman (CFEL, DESY)

J. Gaudin (Bordeaux U.), L. Juha (FZU, Prague)

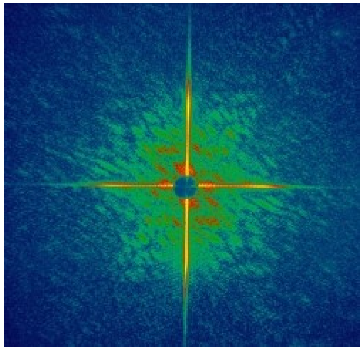

Ch. Gutt (U. Siegen), G. Gruebel, L. Mueller (DESY)

M. Harmand (LULI,CNRS), M. Cammarata (U. Rennes)

S. Hau-Riege (LLNL)

H. Jeschke (U. Frankfurt)

R. Riedel, F. Tavella (DESY)

A. Mancuso, H. Sinn (EXFEL)

S. Toleikis (DESY)

J. Wark, S. Vinko, O. Ciricosta (Oxford U.)

K. Ueda (SACLA)

and ...

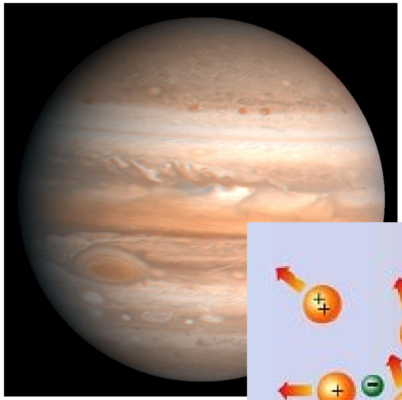

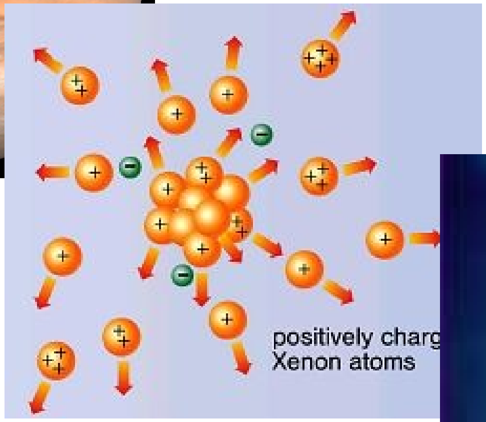

HELMHOLTZ ASSOCIATION

CFEL SCIENCE

DESY

Thanking CFEL Theory Division ...

Z. Jurek

Z. Li

M. A. Malik

N. Medvedev

R. Santra

S.-K. Son

V. Saxena

V. Tkachenko

Members of the CFEL Theory Division: Y.-J. Chen, O. Geffert, Z. Jurek, Y. Hao, K. Hanasaki, A. Hanna, M. A. Malik, A. Karamatskou, Z. Li, N. Medvedev, P. K. Mishra, S. Pabst, D. Popova, R. Santra (Division Director), V. Saxena, J. M. Slowik, S.-K. Son, V. Tkachenko, O. Vendrell, B. Ziaja

HELMHOLTZ ASSOCIATION

CFEL SCIENCE

DESY

Thank you for your attention !